NADH regenerated using immobilized FDH in a continuously supplied reactor – Application to L-lactate synthesis

J. Roche [1], K. Groenen-Serrano, O. Reynes, F. Chauvet, T. Tzedakis *

Laboratoire de Génie Chimique, Université de Toulouse – Paul Sabatier, 118, route de Narbonne, 31062 Toulouse, France

HIGHLIGHTS

- Kinetic of the NADH regeneration using immobilized FDH was examined.
- Kinetic parameters of the enzymatic regeneration of NADH were determined.
- Optimization of the FDH immobilization by encapsulation, was achieved.
- We achieve 3 weeks of continuous synthesis of L-lactate using *in situ* regenerated NADH.
- We simulate the filter press reactor and propose NAD+ diffusivity into a chitosan polymer.

Keywords:
Formate dehydrogenase immobilization
Chitosan
NADH regeneration
Filter press reactor
L-lactate synthesis
NAD^+ diffusion coefficient

ABSTRACT

The present study deals with the design and optimization of a reduced-scale filter press reactor, containing an immobilized layer of formate dehydrogenase between two layers of chitosan, dedicated to the enzymatic synthesis of chiral molecules. Elaboration and optimization of the overall system was carried out to demonstrate the feasibility of the immobilization of formate dehydrogenase in a continuous synthesis process. The results demonstrate that the immobilized FDH keeps half of its enzymatic activity for practically two weeks. In addition, the polymeric matrix allows transfer of NAD^+ with relatively high diffusion coefficients (2.1×10^{-11} m^2 s^{-1}). Experimental validation of NADH regeneration was achieved for pyruvate reduction to L-lactate. Simulation demonstrated that it is possible to achieve practically quantitative conversion of the NAD^+ if the reaction channel reaches a length of half a meter.

1. Introduction

The cofactor nicotinamide adenine dinucleotide (NAD) and especially its reduced form NADH are involved in several reactions catalyzed by dehydrogenase group enzymes (more than 300 dehydrogenases require this coenzyme [1,2]) and lead to optically active compounds (enantiomeric excess of more than 99%), with high added value. However, the high cost of NADH cofactor (>50 k€/mol) does not allow its use in stoichiometric amounts during syntheses, and implies its regeneration *in situ* during the reaction. On the other hand, using an enzyme as catalyst for the syntheses of valuable adducts (e.g. formate dehydrogenase), implies using it in catalytic amounts (classically of the order of the $\mu mol\ L^{-1}$), if economically realistic processes are to be proposed.

Numerous attempts to develop an efficient NADH regeneration process can be found in the literature, but none are industrially satisfying: chemical [3–5] and photochemical methods [6,7], electrochemical or electroenzymatic [8–15] methods, as well as enzymatic or biochemical methods [16–20]. Most often, authors conclude to an incomplete regeneration of NADH, or the regeneration of enzymatically inactive NADH. To qualify as efficient an NADH regeneration method as to lead to a total turnover number (mol of product/initial number of mol of cofactor) in the range 10^3–10^5 while the methods proposed do not reach these performances [21].

When NADH is regenerated electrochemically [15] directly at the electrode in aqueous or non-aqueous media at very cathodic potentials (−0.5 to −1.8 V/SCE) the reaction leads to enzymatically inactive products [22]. Electroregeneration of enzymatically active NADH or NAD(P)H can also be performed indirectly by using a redox mediator for electron transfer [13]. Various redox mediators (methyl viologen, flavins, quinonic compounds, rhodium complexes and some ferrodoxins), assisted by various enzymes (ferrodoxin-$NAD(P)^+$-reductase [23], formate dehydrogenase

* Corresponding author. Tel.: +33 (0)5 61 55 83 02; fax: +33 (0)5 61 55 61 39.
E-mail address: tzedakis@chimie.ups-tlse.fr (T. Tzedakis).
[1] Current address: Institut des Sciences Moléculaires, UMR 5255 Groupe Nanosystèmes Analytiques, Université Bordeaux 1 Site ENSCBP, 16 Avenue Pey Berland, 33607 Pessac, France.

http://dx.doi.org/10.1016/j.cej.2013.10.096

Nomenclature

a	height of the reactor channel, including thickness of the flow stream, the matrix and the enzyme layers $2e_1 + 2e_2 + h$
$C°$, C_j	inlet/initial and outlet concentrations of species j (mol m^{-3})
D_j D_{aj}	diffusion/apparent diffusion coefficient of species j (m^2 s^{-1})
d_h	hydraulic diameter of the flowing channel = 4 ∗ channel section/channel perimeter (m)
E_A	enzyme activity %
e_i	thickness (in z axis) of the various enzymatic and matrix layers, within the microreactor
E_U	enzyme units, here units of FDH: the quantity of enzyme that transforms 1 μmol/min of NAD^+ at 25 °C
FDH	formate dehydrogenase from *Candida boidinii*
f_{NADH}	flux density of NADH produced (mol/h/m^2 of immobilized FDH)
F_v	force applied to the fluid per volume unit
h	thickness (in z axis) of the flowing compartment, within the microreactor
K_{ia}	the dissociation constant of the enzyme-substrate 1/NAD^+' complex, (mol L^{-1})
K_{m1}, K_{m2}	Michaelis constants for substrates S_1 and S_2 respectively, here NAD^+ and $HCOO^-$; (mol L^{-1})
L	reactor channel length in the y axis (m)
LDH	L-lactate dehydrogenase
NAD^+/NADH	oxidized and reduced forms of the nicotinamide adenine dinucleotide cofactor
p	pressure (bar)
Q, Q_R	inlet and recycled volumetric flow rate within the microreactor (m^3 s^{-1})
R	recycling ratio (=Q_R/Q)
Re	Reynolds number ($\rho u\ d_h/\mu$)
S_1 *and* S_2	the first and the second substrate (here NAD^+ and $HCOO^-$) respectively to be linked to the enzyme, to form the Enzyme-S complex
r, r_m, r_j	initial rate, maximum rate and rate defined versus species j respectively, for the enzyme reaction (mol m^{-3} s^{-1})
T	absolute temperature (K)
$\vec{u}$,u_Z, u_y	the fluid velocity vector, and the velocity components in directions z and y (m s^{-1})
X_j	experimental or simulated conversion rate of species j
y	axis parallel to the flow within the microreactor
z	axis orthogonal to the flow (in the perpendicular direction) within the microreactor
α	width of the flow channel (axial direction, orthogonal to the flow) within the microreactor
ΔP	calculated pressure drop (bar)
μ	fluid dynamic viscosity (Pa.s)
τ	residence time of the solution (s)
ρ	fluid density (kg m^{-3})

[12,24], 2-oxocarboxylate and enolate reductases [25], etc.) have been used. Previous works [12] involving the use of a electrochemical microreactor demonstrate that continuous regeneration NADH from NAD^+, using flavin as redox mediator and a formate dehydrogenase enzyme, can be achieved with conversion yields reaching 50%. Nevertheless, the total turnover number and the turnover number (mol of product/initial number of mol of cofactor x operating time) remain lower than 1000 and 100 respectively. On the other hand stability of some of the mediators tested is relatively low, and owing to their toxicity, they are not suitable for chiral synthesis.

For the various kinds of synthesis indicated above, most often the enzyme was used 'free' in solution, thus a large quantity is required, which does not favour an economically valid process.

Attempts to immobilize the enzyme to achieve regeneration of the NADH decreased the enzyme activity, or shortened its lifetime (for example, immobilization of the pair lipoamide dehydrogenase/methyl viologen [11] to produce D-lactate). Nevertheless in a few cases immobilization of enzyme enhanced its activity (for example immobilization of glucose oxidase within a Nafion or chitosan polymeric matrix [26,27]). For other authors [28] immobilization of the enzyme protects it against various aggressive agents or operating conditions (higher temperatures, pH far from optimum, concentrated media or organic solvents).

To our knowledge there are no chemical or electrochemical reactors operating on a pilot or industrial scale able to continuously produce NADH. Usually, this cofactor is produced by biotechnological processes, which are relatively long and require several separation steps; moreover these processes involve complex mixtures, incompatible with continuous regeneration of NADH, used to synthesize various valuable chemicals.

After previous work on the indirect electro-enzymatic regeneration of NADH, using formate dehydrogenase (FDH) from *Candida boidinii* free in solution, the present work aimed to drastically reduce the quantity of enzyme required, in order to propose an improved and optimized process. The study covered the stages from enzyme immobilization to the process implementation, and focused on developing an efficient *in situ* NADH regeneration pathway, in a continuous flow filter-press reactor. The goal was to immobilize FDH in the 'reactor wall' of the flowing compartment and achieve satisfactory conversions for the NADH regeneration. The *in situ* synthesis of L-lactate from pyruvate was chosen as model reaction. The challenge here is to achieve a long time life and satisfactory activity for the FDH, in order to validate the feasibility of the continuous synthetic process at the lab scale. The behavior of this system was studied and optimized both experimentally and through theoretical simulation of the concentration profiles within the reactor to predict conditions allowing the complete conversion of the model substrate, here pyruvate.

2. Experimental section

2.1. Chemicals and devices

Deionized water 18 MΩ was used for all solutions. The chemicals were of analytical grade (purity >98.5%): FDH and medium molecular weight chitosan were from Sigma–Aldrich and NAD^+ from Acros Organics. Formate, Pyruvate, rabbit muscle L-lactate dehydrogenase K_2HPO_4 and KH_2PO_4 were all from Sigma–Aldrich.

NADH, NAD^+, pyruvate and L-lactate concentrations were determined by UV–vis spectroscopy and HPLC according methods described in previous works [12].

2.2. Kinetic studies

To determine the rate equation of the reaction (1) were carried out in a UV–visible cell and absorbance of the NADH produced by reaction (1) was followed at 340 nm.

Pyruvate and L-lactate concentrations were determined by Agilent 1200 HPLC, operated with a UV diode bar detector, at 210 nm and using a PL Hi-Plex H column from Polymer Laboratories and sodium acetate as internal standard. Conditions are described in [12].

2.3. FDH immobilization

A macroporous polymer, alkylchitosan, was used as polymeric matrix for the immobilization of FDH from *Candida boidinii*. The following experimental procedure to prepare the macroporous polymer butylchitosan was used: 0.5 g of 100% deacylated chitosan was added to 15 ml of methanol and 15 ml of 1% acetic acid. The resulting mixture was stirred until a homogeneous gel was obtained. Then, 15 ml of butyraldehyde, followed by 0.7 g of sodium cyanoborohydride were added and the resulting mixture stirred for 10 min. The butylchitosan produced was separated under vacuum filtration and washed 5 times with 25 ml of methanol.

In order to immobilize the FDH, the solid butylchitosan was dispersed in chloroform (1% wt) with an ultraturax. A volume of 60 μL cm^{-2} of the metastable suspension obtained, was spread on the flat support; evaporation of the solvent gave the 1st layer of polymer. A volume of 30 μL cm^{-2} of a FDH solution in ultrapure water, was spread on the coating and after drying, a second layer of polymer was laid on the enzyme deposit, protecting it and avoiding leakage of catalyst into the reaction medium. The resulting structure was washed several times with a fixed volume (the same for all washings) of phosphate buffer pH 7 and the resulting solution was analyzed for the presence of free enzyme. This operation was pursued until the washing buffer no longer contained enzyme.

Experiments on the effects of the various parameters e.g. the immobilization of the FDH, the evaluation of both its immobilized quantity and its optimal load in the butyl alkylchitosan, as well as the stability/life time of the immobilized FDH, were carried out in a stirred phosphate buffer solution, containing 0.5 mmol L^{-1} NAD^+ and 0.1 mol L^{-1} $HCOO^-$.

3. Results and discussion

3.1. Kinetic studies and design of the reactor containing the immobilized enzyme

Several kinetic measurements were carried out, in order to evaluate the various parameters of the kinetic of the enzymatic regeneration of NADH. The reaction of NADH regeneration (1) from NAD^+ uses formate dehydrogenase (FDH), an enzyme whose natural substrate is formate (or methanoate, $HCOO^-$). This reaction obeys a bi–bi ordered mechanism (Theorell–Chance [12,29–30] according to Michaelis–Menten theory and its initial rate r follows relation (2). Linearization of Eq. (2) leads to the Lineweaver–Burk Eq. (3), which allows the determination of the kinetic parameters of the system.

$$NAD^+ + HCOO^- \overset{FDH}{\leftrightarrow} NADH + CO_2 g \quad (1)$$

$$r/r_m = [S_1]\cdot[S_2]/(K_{ia}\cdot K_{m2} + K_{m2}\cdot[S_1] + K_{m1}\cdot[S_2] + [S_1]\cdot[S_2]) \quad (2)$$

$$r_m/r = 1 + K_{m2}/[S_2] + K_{ia}\cdot K_{m2}/([S_2]\cdot[S_1]) + K_{m1}/[S_1] \quad (3)$$

where r_m is the maximum reaction rate, $[S_1]$ and $[S_2]$ are the concentration of the first (NAD^+) and the second ($HCOO^-$) substrate to be linked to the enzyme respectively, to form the Enzyme-S complex, K_{ia} is the dissociation constant of the enzyme-S_1 complex, K_{m1} and K_{m2} are the Michaelis constants of NAD^+ and formate respectively.

Various kinetic measurements were performed by UV–vis spectrophotometry in order to determine the initial reaction rate for different initial concentrations of both substrates NAD^+ and formate. The results were indicated in Fig. 1.

Reproducible UV–visible spectra were obtained enabling follow the absorbance at 340 nm, which is specific of the NADH produced (ε = 5164 M^{-1} cm^{-1}). Several evolutions of $A = f(\text{time})$ are presented in Fig. 1(a), indicating that the evolution is reproducible, and enabling easy initial rate determination. The graph (b) Fig. 1 indicates a linear evolution of the reverse of the reaction rate versus the reverse of the concentration of NAD^+ ($1/r = f(1/[S_1])$), for various formate (S_2) concentrations. The linearity of those evolutions confirms the assumed Theorell–Chance [12,29,30] mechanism, and allows to do the following comments:

i/The graph shows that for a particular value of the NAD^+ concentration '$[S_1]_p$' the rate r becomes independent of the second substrate concentration '$[S_2]$', and all lines $1/r = f(1/[S_1]_p)$ converge to the same point ($1/r_p$, $1/[S_1]_p$), enabling K_{ia} to be determined. Indeed at this particular value ($1/[S_1]_p$), Eq. (3) can be written for two different concentrations ($1/[S_2]_a$ and $1/[S_2]_b$) as follow:

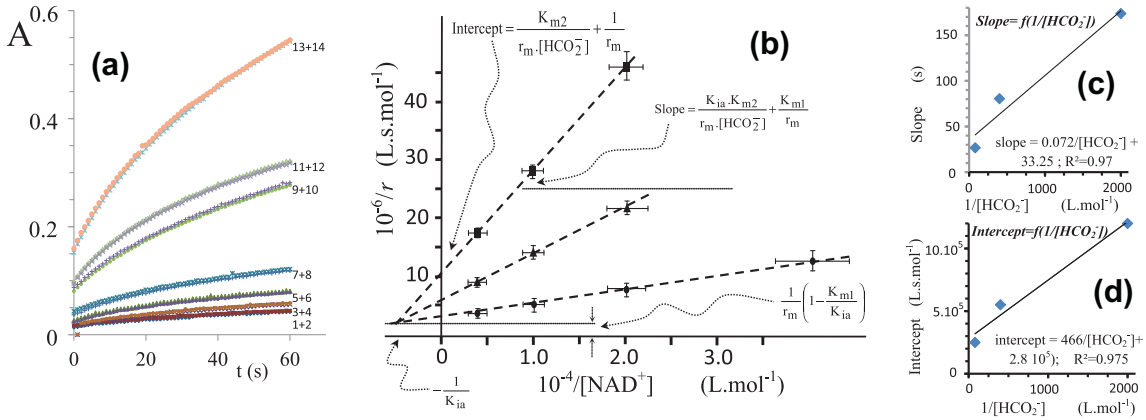

Fig. 1. Experimental results of the kinetic studies carried out on the reaction (1). (a) Several measurements of the absorbance (at 340 nm/NADH) versus time (checked twice) 1 + 2: [Formate] = 0.5 mM; [NAD^+] = 25 μM; 3 + 4: [Formate] = 0.5 mM; [NAD^+] = 50 μM; 5 + 6: [Formate] = 2.5 mM; [NAD^+] = 25 μM; 7 + 8: [Formate] = 2.5 mM; [NAD^+] = 50 μM; 9 + 10: [Formate] = 2.5 mM; [NAD^+] = 250 μM; 11 + 12: [Formate] = 12.5 mM; [NAD^+] = 100 μM; 13 + 14: [Formate] = 12.5 mM; [NAD^+] = 250 μM. (b) The reverse of the reaction versus the reverse of the substrate 1 (NAD^+) concentration (according to the Lineweaver–Burk plot e.g. a bi–bi ordered mechanism). FDH from *Candida boidinii* 0.79 E_U m L^{-1} in phosphate buffer pH = 7.0; T = 38 °C. [HCO_2^-]: (■) 0.5 mM; (▼) 2.5 mM; (●) 12.5 mM. (c) Slopes of the straight lines of the graph (b) versus the reverse of the substrate 2 (HCO_2^-) concentration. (d) Intercepts of the straight lines of the graph (b) versus the reverse of the substrate 2 (HCO_2^-) concentration.

$$1/r_p = 1/r_m + K_{m2}/(r_m \cdot [S_2]_a) + ((K_{ia} \cdot K_{m2}/(r_m \cdot [S_2]_a)) + K_{m1}/r_m)/[S_1]_p = 1/r_m + K_{m2}/(r_m \cdot [S_2]_b) + ((K_{ia} \cdot K_{m2}/(r_m [S_2]_b)) + K_{m1}/r_m)/[S_1]_p \Rightarrow 1/[S_2]_a + K_{ia}/([S_1]_p \cdot [S_2]_a) = 1/[S_2]_b + K_{ia}/([S_1]_p \cdot [S_2]_b) \Rightarrow - 1/[S_1]_p = 1/K_{ia} \quad (3a)$$

Moreover taking into account the Eq. (3a), one can see that the rate r at the particular value $(1/[S_1]_p)$, becomes independent of the second substrate concentration '$[S_2]$', as indicated below (3b):

$$(1/r_p)\ at\ [S_1]_p = 1/r_m - K_{m1}/(r_m K_{ia}) \quad (3b)$$

ii/the evolution of the slope $\frac{K_{ia} \cdot K_{m2}}{r_m \cdot [HCO_2^-]} + \frac{K_{m1}}{r_m}$ of curves $1/r = f(1/[S_1])$ in (graph (b), Fig. 1), versus the reverse of the concentration of formate $(1/[S_2])$, appears to be linear (graph (c); slope = 0.0715/$[HCO_2^-]$+33.25); $R^2 = 0.97$).iii/in a similar manner, the evolution of the intercept $\frac{K_{m2}}{r_m [HCO_2^-]} + \frac{1}{r_m}$ of curves $1/r = f(1/[S_1])$ in (graph (b), Fig. 1), versus the reverse of the concentration of formate $(1/[S_2])$, appears to be linear (graph (d); intercept = 466/$[HCO_2^-]$ + 2.8 × 10^5; $R^2 = 0.975$). This last equation directly provides the value of the maximum rate of the enzymatic reaction r_m (intercept) and allows determination of the second Michaelis constant K_{m2}. Then from the equation of the graph (c), K_{m1} can be deduced and K_{ia} can be verified. All these kinetic parameters, were summarized in Table 1; they were used to simulate the concentration profile in the reactor.

Note that strong deviations were observed for the determined values of these various parameters. Max/mini deviations were evaluated and the corresponding uncertainties indicated in the table. In some case uncertainty reaches 60%.

3.2. Immobilization of formate dehydrogenase: principle and characterization

Using an enzyme as catalyst for the syntheses of valuable adducts, implies its use in catalytic amounts (classically of the order of μmol L^{-1}), to make the processes economically realistic. One way to reach this goal is to fix the enzyme required within an inert support to create conditions allowing high enzymatic activity as well as a long life time. Formate dehydrogenase is very sensitive to its environment and thus a few methods for its immobilization have been developed with satisfactory enzyme activity and stability [31,32].

Chitosan is a derivative of chitin, a natural polysaccharide, extracted from the shells of arthropods (Fig. 2). This polymeric structure, synthesized since the 80s [33], allows the diffusion of reagents from the solution; its first application 'as enzyme host' was studied for biofuel cell applications [26]. In this study, a 'medium molecular-weight' chitosan was used to prepare butylchitosan according to the reaction scheme in Fig. 2.

The support/surface chosen for the experiments was a microstructured gold plate, which can be inserted in a filter-press reactor. The plate, presented 130 semi-cylindrical channels in the y direction; each channel can be assumed to be an ideal plug flow reactor, and can be used as a high specific area electrode. The gold plate was chosen here with a view to other applications involving different mediators, for instance used in indirect enzymatically assisted electrochemical regeneration. Here, the microchannels improve the adherence of the polymeric matrix. The ratio between the size of the microchannel and the thickness of the overall immobilized layer was in the range from 3 to 5. A 'layer-by-layer' type configuration was chosen for the immobilization of FDH, as shown in Fig. 3, which also indicates the overall reaction scheme of L-lactate synthesis from pyruvate.

Table 1
Kinetics parameters of reaction (1), extracted from the results in Fig. 1, according to Eqs. (2) and (3). The formate dehydrogenase was extracted from *Candida boidinii*.

r_m (mol L^{-1} s^{-1})	K_{ia} (mol L^{-1})	K_{m1} (mol L^{-1})	K_{m2} (mol L^{-1})
(4 ± 2).10^{-6}	(1.5 ± 0.3) 10^{-4}	(14 ± 6) 10^{-5}	(3 ± 2) 10^{-3}

The top of the deposit was not smooth, the roughness (double the average thickness of the deposit) exists on the surface of the gold plate. For this preliminary work, we assumed that the thickness of the various layers was constant, and when reported, the thickness corresponds to the average value.

The functionalized plate was washed as described above; the fraction of enzyme removed from the washed plate was evaluated by mixing the washing solution with the phosphate buffer solution containing NAD^+ and $HCOO^-$. Reaction (1) occurs, and the absorbance was monitored at 340 nm, to detect NADH produced. UV–visible spectra allow the determination of the initial rate of the reaction (1), as well as the fraction of enzyme removed, at each washing (Fig. 4).

The results show that, during the 5 washings, 20% of the initially introduced enzyme was removed into the buffer solution. During the 6th washing, no enzyme was detected (<1% of the initial involved quantity of FDH). These results were reproducible (checked repeatedly).

The quantity of enzyme (FDH) in the immobilization matrix can be varied by changing the concentration of the enzyme solution. In order to determine optimal enzyme loading, the functionalized and washed plate was immersed, for 1 h, in a stirred phosphate buffer solution containing NAD^+ and $HCOO^-$. The NADH produced from reaction (1) was quantified by UV–visible spectrophotometry at 340 nm and the results are presented in Fig. 5 indicating the concentration of NADH as a function of the number of enzymatic units (E_U) of FDH initially introduced within the polymer. Note that 'one enzymatic unit (E_U)' of FDH is defined as the quantity of enzyme that allows the transformation of 1 μmol min^{-1} of NAD^+ at 25 °C. For low enzyme contents (<0.8 E_U) the concentration of NADH produced increased as a function of the number of FDH units initially introduced, indicating a chemical rate dependent on the immobilized catalyst activity.

For higher FDH loading in the polymer, the concentration of NADH produced reaches a plateau, meaning either that diffusion through the polymeric matrix becomes limiting or that maximum enzyme loading has been reached. For this kind of polymer, the optimum catalytic activity of the functionalized plate corresponds to a loading of enzyme of 0.72 E_U (24 E_U g^{-1} of polymer), a value relatively low in comparison with the free enzyme content usually reported in solution [12].

3.3. Optimization of continuous NADH regeneration in a filter press reactor

Two plates containing the immobilized FDH, were used as interfaces of the 'one-flow' compartment of the filter-press microreactor (Fig. 6, designed and optimized in previous works [12]) in order to optimize the continuous regeneration of NADH, using formate as co-substrate. A Teflon plate was used to define the thickness of the flowing compartment.

3.3.1. Study of the life time of the immobilized FDH

In order to examine the stability of the immobilized enzyme, a three-week continuous operation (NADH production) was carried out. The reactor was thermoregulated at 38 °C and the reaction mixture, containing NAD^+ and $HCOO^-$ in phosphate buffer, flowed at 63 μL min^{-1}. The concentration of NADH produced was continuously monitored at the outlet of the reactor by UV–vis

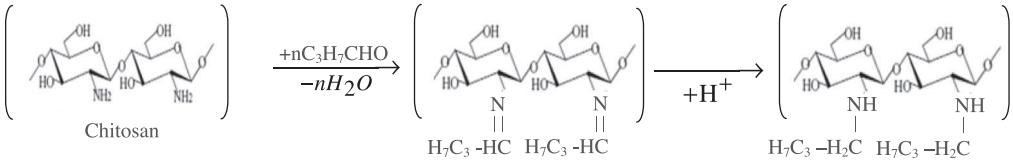

Fig. 2. Structure of chitosan and reaction scheme of its functionalization.

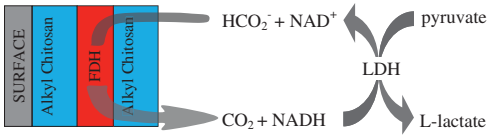

Fig. 3. Schematic representation of the enzymatic regeneration of NADH using formate dehydrogenase (FDH) coupled to a model enzymatic reaction, namely L-lactate synthesis from pyruvate catalyzed by L-lactate dehydrogenase. The enzyme was immobilized in an alkyl modified chitosan matrix according to a 'layer by layer' structure.

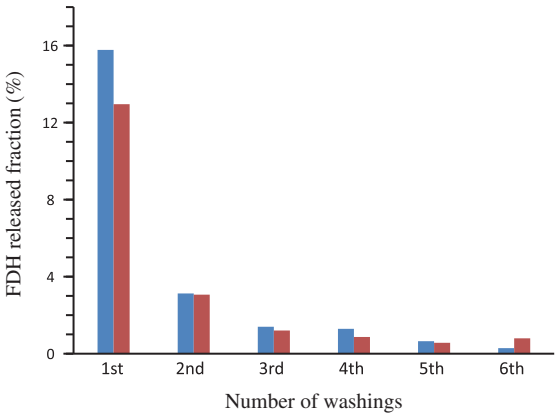

Fig. 4. Removed fraction of the initially introduced enzyme from the washed (using phosphate buffer pH = 7) functionalized plate, as a function of the number of washing steps. Enzyme quantity was determined by assay of the NADH produced, by HPLC measurements; the amount of FDH present in solution was determined using the kinetic law. This curve corresponds to the FDH obtained for the optimized enzyme quantity (0.72 U) with two different FDH enzyme lots. Other experimental conditions are described in Section 2.

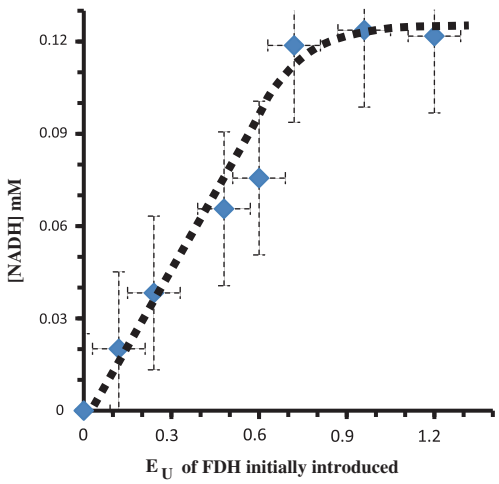

Fig. 5. Concentration of NADH produced at 38 °C by reaction (1) as a function of the quantity of initially introduced FDH (E_U). Reaction duration 1 h; FDH immobilized in a 'butylchitosan macroporous polymer' coated at a microstructured plate, submitted to 5 washing process; $[NAD^+]° = 0.5$ mmol L^{-1}; $[HCOO^-]° = 0.1$ mol L^{-1}.

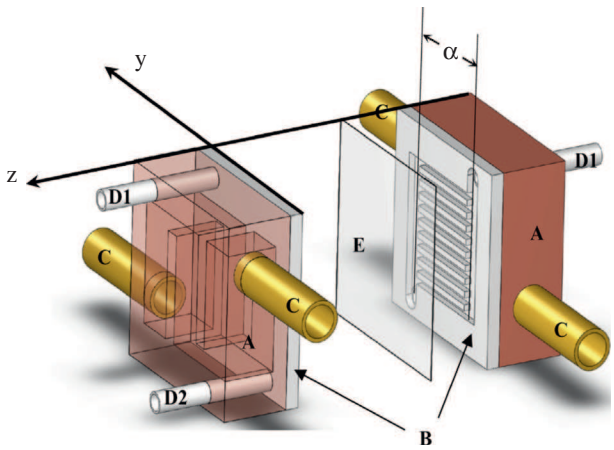

Fig. 6. Microstructured filter-press reactor. (A) Thermal exchanger; (B) Microstructured plate (containing 130 semi-cylindrical micro-channels of 160 μm diameter) coated with immobilized FDH; (C) Inlet and outlet of heating fluid; (D1, D2) Reaction mixture outlet and inlet; (E) Ion exchange membrane (optional).

spectrophotometry at 340 nm. Fig. 7 presents the results, as the percentage of the enzyme activity (E_a) versus time. It can be seen that the enzyme activity remained over 50% for 2 weeks and after 3 weeks, 30% of enzyme was still active. The flux density of the NADH produced was in the range 0.140 mmol h^{-1} m^{-2} at the initial time, to 0.050 mmol h^{-1} m^{-2} after three weeks, so a good performance. Comparison with other studies ([12], a kind of indirect electrochemical regeneration of NADH using flavin, involving free FDH in solution and applied for L-lactate synthesis or in other studies involving biphasic media [32]) is difficult: indeed, for our previous experiments, runs performed in similar conditions ($[NAD^+] = [pyruvate] = [flavin]$ 4 mM and high concentration 0.5 E_U/cm^3 of FDH) led to higher production of L-lactate (0.12 mol m^{-2} J^{-1}), but recovery of the enzyme from the outlet solution was difficult and its residual activity was not evaluated.

3.3.2. Influence of the flow rate on continuous NADH production

Plates modified with the optimized enzyme loading and washed were used to examine the effect of the various operating parameters on NADH production in a continuous process. The filter press reactor used contains the two microstructured plates coated with butylchitosan/FDH as previously described. Fig. 8 presents the influence of the volumetric flow of the feed mixture (containing NAD^+ and $HCOO^-$ in phosphate buffer) on the NADH produced versus time; analyses were performed on the solution collected at the outlet of the reactor and cumulated for 15 min.

The curves (Fig. 8(A)) show that the system requires about half an hour (in the range of flow rates chosen) to reach the steady state, thus for longer times, the NADH concentration, as well as the NAD^+ conversion, became constant. At the steady state, the conversion of NAD^+ decreased from 15% to 5% while the Reynolds number increased from 6.4 to 38.7 (e.g. flow from 63 to 380 μL min^{-1}).

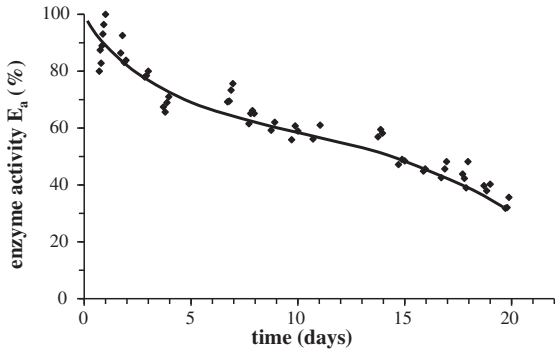

Fig. 7. Percentage of initial enzymatic activity (E_a) as a function of the duration of the continuous operation. Inlet solution: $[NAD^+]^\circ$ = 0.5 mmol L^{-1}, $[HCOO^-]^\circ$ = 0.1 mol L^{-1} in phosphate buffer pH = 7, Q = 63 μL min^{-1}, T = 38 °C.

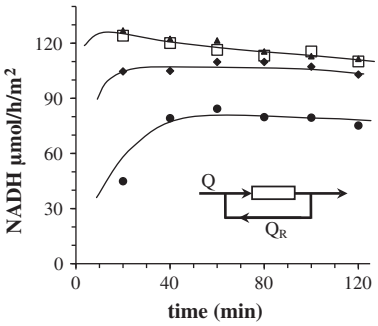

Fig. 9. NADH production (μmol/h/m^2 of immobilized FDH) versus time, for various (4) recycling ratios ($R = Q_R/Q$). For the initial feed solution: flow Q: 63 μL min^{-1}; NAD^+ 0.5 mmol L^{-1}; $HCOO^-$ 0.1 mol L^{-1} in phosphate buffer pH 7; 38 °C. ● R = 0/no recycling; □ R = 1; ▲ R = 3; ♦ R = 5. Inset: Schematic view of the filter press reactor including a recycling flow.

This result calls for two comments:

- increasing the flow caused both the residence time and consequently the conversion of NAD^+ to decrease,
- on the other hand, increasing the flow acted on the NAD^+ transfer especially at the polymeric matrix/solution interface and tended to overcome external (to the matrix) diffusion limitation. To conclude, the decrease in the conversion indicates either a strong internal (to the matrix) diffusion limitation or a chemical kinetic limitation.

Fig. 8(B) presents the time dependency of the cumulated production of NADH (f_{NADH} μmol m^{-2} h^{-1} of immobilized FDH), for the same range of flow rates.

In spite of a certain dispersion of the results (uncertainty on the volume, especially for low flows), increasing the flow led to higher production of NADH, even if conversion of NAD^+ remained lower than 20%. Some specific points to improve are:

- some dead volumes exist within the reactor, so the overall shape and geometry of the microstructured plates has to be improved; this work is in progress at the laboratory;
- besides the reactor shape, the immobilization matrix of butylchitosan presents a high hydrophobicity, interacting with and retaining stagnant bubbles, especially in the dead volumes of the compartment. Increasing the flow removes the air from the polymer, thus increasing the active surface area of the interface. Nevertheless, this seems to be minor in comparison with either the chemical kinetic limitation arising from the quantity of immobilized FDH, and internal (within the matrix) diffusion limitation.

3.3.3. Influence of the recycling ratio R on the continuous production of NADH

For a better understanding of this system and to progress in the identification of the limiting steps in the regeneration of NADH, the influence of continuous recycling of the reaction mixture was examined. A fraction R, the so-called recycling ratio ($R = Q_R/Q$) of the outlet flow was injected back at the inlet. Fig. 9 shows the production of NADH versus time of reaction for various recycling ratios. The chosen feed flow Q corresponds to the lowest flow previously (Fig. 8) used, in order to simultaneously examine the effect of any dead volumes within the reactor.

The results call for the following remarks:

(i) the steady state production of NADH significantly increases ($75 < f_{NADH}$ in μmol/h/$m^2 < 110$) when solution was recycled (R going from 0 to 1), especially for low recycling ratios. Indeed, increasing the flow reduces the dead volumes of the reactor; in fact the whole surface of the butylchitosan layer containing the immobilized FDH was in contact with fresh solution;

(ii) the system reached the steady state faster (~20 instead ~40 min) when solution was recycled, probably for the same reasons as in (i);

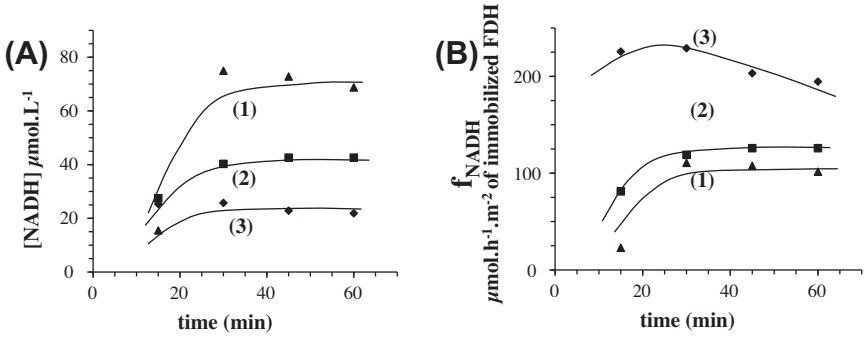

Fig. 8. Time dependence of the NADH produced for various volumetric flows. Inlet solution: NAD^+ 500 μmol L^{-1}; $HCOO^-$ 0.1 mol L^{-1}; phosphate buffer pH = 7.0; 38 °C. (1) to (3) respectively 63, 127 and 380 μL min^{-1}. Analyses were performed on the solution collected at the outlet of the reactor and cumulated for 15 min. (A): Outlet concentration of NADH; (B): production of NADH.

(iii) an additional increase in the flow within the reactor ($R > 1$) seems to have a minor effects on NADH production. Recycling ratios equal to or higher than 1 overcome problems such as dead volumes or wetting the butylchitosan layer;
(iv) The fact that, above a value of 1, R has no effect on the NADH production implies that there is no external limitation to the polymeric matrix diffusion. Consequently, limitation of NADH production seems to be caused either by mass transfer limitation through the polymer (internal diffusion), or by the kinetics of the enzyme reaction;
(v) higher recycling ratios ($R \geqslant 5$) seem to have a negative effect on NADH production which decreases, probably because friction is delaminating the matrix from the metallic support.

3.3.4. Application of NADH regeneration to the L-lactate synthesis

The final goal of our project was to develop an economically efficient regeneration process for the cofactor NADH that can be used *in situ* during various enzymatic syntheses. Various NADH regeneration approaches exist though many [9] are known to lead to enzymatically inactive NADH. In order to check the reactivity of the regenerated NADH and to verify that this regeneration process can be used *in situ*, the synthesis of L-lactate from pyruvate catalyzed by L-lactate dehydrogenase (LDH) was coupled with this system, as a model enzymatic reaction, consuming NADH (4).

$$CH_3COCOO^- + NADH + H^+ \xrightarrow{LDH} CH_3C^*HOH - OCOO^- + NAD^+ \quad (4)$$

The kinetics of this reaction obeys an ordered Theorell–Chance mechanism:

$$r_4 = k_4 \cdot [LDH]^\circ / (1 + K_{\text{mixed inhibition constant NADH}-\text{pyruvate}} + K_{m\ \text{NADH}}/[NADH] + K_{m\ \text{pyruvate}}/[\text{pyruvate}])$$

the reaction is fast and total [12], the enzyme LDH is commercial and stable and the L-lactate produced, can be easily quantified by HPLC.

The filter press reactor, previously functionalized with immobilized formate dehydrogenase, was used to perform syntheses at 38 °C; the reactor was supplied by a solution of phosphate buffer containing the cofactor NAD^+, formate, the enzyme LDH, as well as the pyruvate at 2 different concentrations. The outlet flow was collected, analyzed by HPLC (detection of pyruvate and lactate, [12]) and the solution injected back into the reactor three times, in order to increase the conversion rate and to simulate a series of successive reactors.

Table 2 summarizes the results, i.e. the pyruvate conversion for two different initial concentrations and for 3 runs in the reactor. The relatively low conversions (16–27%) after one residence time within the reactor, significantly increase (33–59%) after three successive recyclings of the outlet solution.

The L-lactate production demonstrates that the continuous regeneration of enzymatically active NADH was effective. The UV–vis spectrum of the solution obtained at the end of the experiment shows that there was no accumulation of NADH in the system, implying that all the NADH formed is consumed by the model reaction. The NAD^+ conversion rates obtained have to be compared with that obtained without any model reaction: indeed, in the same conditions of flow rate and concentration, 14% of NAD^+ was transformed into NADH whereas 27% was obtained with the model reaction (1st run, for mol per mol reaction). The addition of a second enzymatic reaction that consumes the NADH formed, shifts the equilibrium toward regeneration.

Table 2
Conversion rate of pyruvate to L-lactate after 3 passes (three successive passages) through the reactor. Initial solution: phosphate buffer pH = 7; $[NAD^+] = 0.5$ mmol L^{-1}; $[HCO_3^-] = 0.1$ mol L^{-1}; $[LDH] = 5\ E_U\ ml^{-1}$; $T° = 38$ °C; flow rate 63 µL min^{-1}.

	Conversion rate of pyruvate (%)		
[pyruvate]/mmol L^{-1}	1st run	2nd run	3rd run
1	16	26	33
0.5	27	44	59

3.4. Theoretical analysis of the overall enzymatically catalyzed synthetic process

3.4.1. Simulation of the concentration profile

Limitation in NADH (or pyruvate) conversion rate in the continuous process can be caused by three different phenomena: the external diffusion of reagents in solution, the internal diffusion of reactants in the immobilization matrix and finally the chemical reaction (1). Since increasing convection *via* recycling the solution does not increase production, external diffusion limitation was not limitative. For a better understanding of this system (see schema in Fig. 10), the mass balance of NAD^+ was established at the steady state and the simulated concentration profiles in the reactor were deduced. The corresponding equations as well as the associated boundary conditions were determined and the resulting system was implemented in COMSOL-Multiphysics.

The coating ($e_1 + e_2$, Fig. 10) was thick compares with the size (opening diameter) of the channels, thus, firstly the system was assimilated to two parallel plates defining a channel of rectangular section. The reaction channel can then be divided into three different areas (according to the z axis, i.e. the width of the flow channel):

Area A represents the flow channel, defined between the functionalized plates. In this area, the fluid velocity is calculated, in the steady state, using a simplified Navier–Stokes equation (Eq. (5)), applied to an incompressible fluid.

$$\rho[(\vec{u}\nabla)\vec{u}] = -\nabla\vec{p} + \mu\nabla^2\vec{u} + F_v \quad (5)$$

where: ρ is the fluid density, p the pressure, μ the fluid viscosity and F_v is the force applied to the fluid per unit volume. Eq. (5) was used to calculate the value of the velocity vector at any point of *area A*.

Area B is the top layer of the butylchitosan matrix coating the enzymatic layer; it does not contain any enzyme, convection was ignored and only internal diffusion of the reagents took place in this area.

Area C is the bottom butylchitosan matrix containing the enzyme layer; chemical reactions take place in this area.

The mass balance was established for the limiting reagent (j) i.e. cofactor NAD^+, the formate being in excess. In the steady state, only convection and diffusion (no migration of NAD^+ without electrical field) govern the NAD^+ motion, thus, mass balance can be described by Eq. (6):

$$\text{div}(-D_j\nabla C_j + u C_j) + r_j = 0 \quad (6)$$

where: r_j is the rate of the enzymatic reaction (1), assumed to be described by Eq. (2) which gives in fact the initial rate of the reaction; D_j and C_j are the diffusion coefficient and the NAD^+ concentration respectively; u is the fluid velocity (m/s).

Note that Eq. (6) can be simplified:

- we assume symmetry in the axial direction, changes in the concentration take place in the orthogonal (z) and longitudinal (y) axes,
- as a function of the area considered, some terms can are ignored, e.g. for *area B* both the convective and the chemical reaction terms; conversely for *area C* only the convective term was ignored.

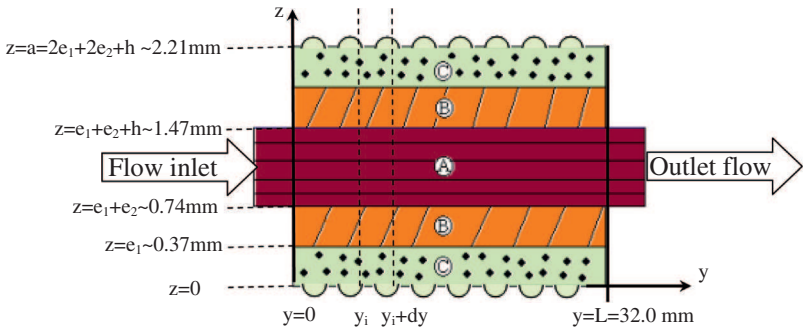

Fig. 10. Schematic geometry of the axial section of the plug flow filter press reactor used to perform simulations. *Area A*: Convection flow between both functionalized plates (section and volume of the flowing channel are respectively: 3.2 cm * 0.074 cm = 0.237 cm^2 and 3.2 cm * 0.074 cm * 3.2 cm (or variable) = 0.757 cm^3). *Area B*: Top layer of the immobilization matrix coating the enzymatic layer. *Area C*: Enzymatic layer.

In *area A*: $Dj\left(\frac{\partial^2 Cj}{\partial z^2}\right) - u_z \frac{\partial C_j}{\partial z} = 0$; In *area B*: $D_j\left(\frac{\partial^2 C_j}{\partial z^2}\right) = 0$; In *area C*: $D_j\left(\frac{\partial^2 C_j}{\partial z^2}\right) - r_j = 0$

Taking account of the concentration profile according axis *z*, the changes in this concentration according to axis *y* (the length of the plug flow/filter press reactor), can be written as follows:

$$D_j\left(\frac{\partial C_j}{\partial z}\right)_{z=0} \alpha\, dy + \alpha u_y h\left(\frac{\partial C_j}{\partial y}\right) dy = r_j \alpha h\, dy \Longleftrightarrow \frac{D_j}{h}\left(\frac{\partial C_j}{\partial z}\right)_{z=0} dy + u_y\left(\frac{\partial C_j}{\partial y}\right) dy = r_j\, dy \quad (7)$$

where α and h are the width and the height of the flow channel respectively.

The following three conditions are required to solve Eqs. (6) and (7) and to find C_j at the solution/chitosan matrix interface ($e_1 + e_2 \leqslant z \leqslant h + e_1 + e_2$) and at the outlet of the reactor, i.e. for $y = L$

(i) $C_{y=0} = C°$

(ii) Flux equality for j between areas B and C:

$$D_j\left(\frac{\partial C_j}{\partial z}\right)_{z=e_1} = D_j\left(\frac{\partial C_j}{\partial z}\right)_{z=e_1+e_2}$$

(iii) Flux for j at $z = 0$ and $z = a = 2e_1 + 2e_2 + h$: $D_j\left(\frac{\partial C_j}{\partial z}\right)_{z=0} = 0$.

3.4.2. Validation of the theoretical model

The diffusion coefficient *D* is the key parameter to govern the limitation of transfer through the immobilization matrix (the butylchitosan layer).

The value of the diffusion coefficient of the NAD^+ in solution was evaluated in the present study [34] by plotting voltammetric curves using a rotating disk electrode and the Levich law. The value determined was 2.4×10^{-10} m^2 s^{-1}, is in agreement with results obtained by Damian et al. [14].

D was used here as the adjustable parameter to check the program, e.g. to compare the theoretical value of the NAD^+ conversion with the experimental one. For initialization of the simulation, the NAD^+ diffusion coefficient in the butylchitosan was taken as the adjustable parameter ($D_{adjusted}$), the other operating parameters being kept constant. Using a $D_{adjusted}$ value equal to the value in solution ($D = 2.4 \times 10^{-10}$ m^2 s^{-1}), led to an overestimation of the simulated conversion of NAD^+ at the outlet of the reactor (e.g. $X_{simulated}$ = 44% instead $X_{experimental}$ = 14% Fig. 8A(1)). Values of $D_{adjusted}$ two order of magnitude lower lead to an underestimation of the simulated conversion of NAD^+ at the outlet of the reactor (e.g. $D_{adjusted} = 2.4 \times 10^{-12}$ m^2 s^{-1} → $X_{simulated}$ < 1% instead $X_{experimental}$ = 14%).

Finally, the value of $D_{adjusted}$ 2.1×10^{-11} m^2 s^{-1} led to a good agreement (simulated conversion/experimental conversion ~1), and was used for other simulations; it was called 'apparent diffusion coefficient' of NAD^+ within the butylchitosan polymeric matrix.

The simulated concentration profile of NAD^+ in the reactor using the apparent diffusion coefficient is reported in Fig. 11. A steep concentration gradient exists in the immobilization matrix, implying that the regeneration of NADH is mainly governed by the internal diffusion of NAD^+ in the butylchitosan layer.

The value of the apparent diffusion coefficient ($D_{aNAD+} = 2.1 \times 10^{-11}$ m^2 s^{-1}) can be compared with values from the literature: e.g. the diffusion of NAD^+ cofactor in electrogenerated polypyrrole membranes leads to an apparent diffusion coefficient of a magnitude of 10^{-15} m^2 s^{-1}, 10,000 fold lower than the present value. This comparison indicates that the immobilization method leads to a porous polymer with a relatively high diffusion of the cofactor.

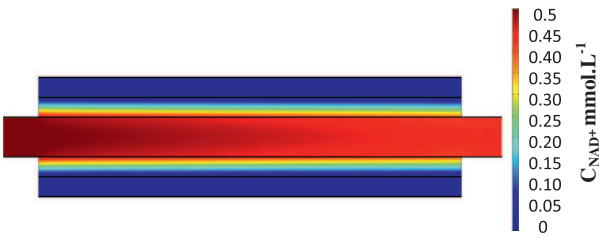

Fig. 11. Simulated concentration profile of NAD^+ in the reactor. $[NAD^+]° = 0.5$ mmol L^{-1}, $[HCO_2^-]° = 0.1$ mol L^{-1}, $T = 38$ °C. Flow rate 63 µl min^{-1}. Apparent diffusion coefficient $D_a = 2.1 \times 10^{-11}$ m^2 s^{-1}.

3.4.3. Simulation of both the effect of the flow and the reaction channel length, on the theoretical conversion of NAD^+

We determined the theoretical optimum parameters (mainly volumetric flow and channel size of the filter press reactor) for the highest conversion of NAD^+. The results are reported in Fig. 12, indicating that NAD^+ conversion (experimental and simulated) is dependent on flow. Note that simulated results are in agreement with experiment, confirming the apparent diffusion coefficient determined above.

Simulation (Fig. 12a) clearly demonstrates that it is possible to reach a quasi-quantitative conversion of NAD^+ for flow rates lower than 10 µL min^{-1} (Re = 1.02, residence time of the solution $\tau = 7.57\ 10^{-7}/(10 \times 10^{-9}/60) = 4546$ s). Experimental verification of this result is difficult with the filter press reactor because of problems such as 'dead volumes/wetting of butylchitosan layer' (§ 3.3.3). Increasing the flow causes a rapid decrease of NAD^+ conversion, because the low residence time does not allow sufficient supply of the enzyme layer with NAD^+ to achieve the chemical reaction, which is limited by the amount of enzyme immobilized. For flow

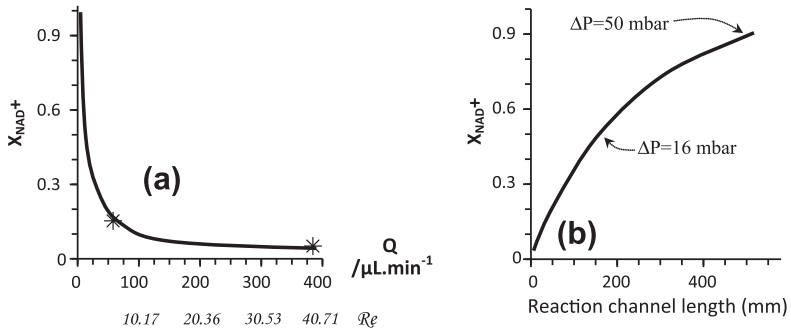

Fig. 12. Simulated conversion of NAD^+ (X_{NAD+}) obtained at the outlet of the reactor versus: (a) the volumetric flow rate and (b) the reaction channel length according to direction y. $[NAD^+]^\circ = 0.5$ mmol L^{-1}, $[HCO_2^-]^\circ = 0.1$ mol L^{-1}, $T = 38$ °C. $D_{NAD+} = 2.1.10^{-11}$ m^2 s^{-1}; channel width = 32 mm. (a) channel length $L = 32$ mm; (✳) experimental results; (b): Flow rate $Q = 63$ µl min^{-1}.

rates higher than 120 µL min^{-1} (Re = 12.2, residence time of the solution $\tau = 7.57 \times 10^{-7}/120 \times 10^{-9}/60) = 379$ s), NAD^+ conversion drops drastically, meaning that the time required for NAD^+ to penetrate the butylchitosan layer is higher (at least the same order of magnitude) than the residence time.

In order to achieve greater conversion of the NAD^+, while maintaining satisfactory flow rates, the effect of the length of the reaction channel was examined. Results (Fig. 12b) show that increasing the length of the reaction channel causes the conversion to increase, because the global flux of NAD^+ arriving at the enzyme layer is higher. When the channel lengths used are of the order of 15 cm, the conversion of NAD^+ becomes higher than 50%, and a 50 cm channel length is required to convert 90% of NAD^+. This will be the expected goal in future works, by using the same type of reactor containing a stack of elementary cells, acting as successive reactors.

Let us note that for the flow channel used here (3.2 cm × 50 cm), and a flow of 63 µL min^{-1}:

- the calculated pressure drop remains lower than 50 mbar;
- the flux density of NADH reaches 0.11 mmol m^{-2} h^{-1} which remains relatively low for production processes. To increase this flux, the amount of immobilized enzyme has to be increased without additional increases of the thickness or the porosity of the polymer.
- the theoretical value of the reaction-channel lengths obtained for high conversions is overestimated since the kinetics law (2) used in the model takes into account the initial rate of the enzymatic reaction (1). In fact, the validity of the reaction rate has to be examined for higher NAD^+ conversion (possible inhibition of the enzyme), so the channel has to be longer than the calculated length.

4. Conclusion

The study, covering the stages between enzyme immobilization to process implementation, allowed the development of an *in situ* NADH regeneration pathway, in a continuous flow filter-press reactor. Formate dehydrogenase was immobilized between two butyl chitosan layers in the 'reactor wall' of the flowing compartment. The main goal was to examine the lifetime and the activity of the FDH, in order to validate the feasibility of the continuous synthetic process at the lab scale. The results demonstrate that the optimum catalytic activity of the functionalized plate corresponds to a maximum enzyme load of 0.72 E_U (24 E_U g^{-1} of polymer), that is lower than the free FDH concentration used in previous works [12] in the range 1–5 E_U/cm^3. A fraction corresponding to 20% of the enzyme initially introduced, was removed in the buffer solution during the 5 required washing steps. The immobilized FDH was continuously regenerating NADH within a reduced scale filter press reactor for 3 weeks; the results showed that enzyme activity remained over 50% for 2 weeks and after 3 weeks, 30% of the enzyme was still active. The flux density of the NADH produced was in the range 0.14 mmol h^{-1} m^{-2} at the initial time, to 0.05 mmol h^{-1} m^{-2}, after three weeks, which is a good performance compared to previous studies [32].

The effects of the flow rate as well as the recycling ratio on the conversion of NADH during continuous production within the reactor were examined. At least 30 min (depending on the Reynolds number) were required to reach the steady state for the NADH concentration which is satisfactory for long-duration operations. Nevertheless NAD^+ conversion rapidly decreased versus flow, the rate-limiting step for NADH production seems to be either mass transfer through the polymer (internal diffusion), or the kinetics of the enzyme reaction.

The *in situ* synthesis of L-lactate from pyruvate was chosen as model reaction. The behavior of the system was studied and optimized experimentally. Experimental results showed it was possible to produce the L-lactate using the *in situ* regenerated NADH. After three successive recyclings of the outlet solution through the reactor, conversion of a 0.5 mmol/L pyruvate solution reached about 60%, which is satisfactory for this reduced scale lab reactor.

In addition, these experimental results were used to check the validity of COMSOL-MULTIPHYSICS based theoretical simulations, by determining an apparent diffusion coefficient for the NADH ($D_{aNAD+} = 2.1 \times 10^{-11}$ m^2 s^{-1}) within the chitosan polymeric layer. This value appears to be relatively high and confirms a certain porosity of the modified polymer compatible with the synthesis process conditions.

Finally these experimental and simulation results show an NADH conversion limited by both internal transfer and the rate of the chemical reaction. In order to achieve higher (∼90%) conversion of NAD^+ while maintaining satisfactory flow rates, simulation indicates that higher channel lengths (∼50 cm) are required. A stack of elementary cells, supplied as successive reactors, is expected, in future work, to overcome the low conversion of NAD^+, at constant enzyme quantity immobilized in the polymer.\

References

[1] M. Dixon, E.C. Webb, C.J.R. Thorne, K.F. Tipton, Enzymes, 3rd ed., Longmans, Green & Co., London, and Academic Press, New York, 1979.
[2] Ze'ev Shaked, G.M. Whitesides, Enzyme-catalyzed organic synthesis: NADH regeneration by using formate dehydrogenase, J. Am. Chem. Soc. 102 (23) (1980) 7104–7105.
[3] P. Wagenknecht, J. Penney, R. Hembre, Transition-metal-catalyzed regeneration of nicotinamide coenzymes with hydrogen, Organometallics 22 (2003) 1180–1182.
[4] C. Stephanson, G. Flanagan, Non-toxic hydride energy source for biochemical and industrial venues: ORP and NAD^+ reduction analyses, Int. J. Hydrogen Energy 29 (2004) 459–464.

[5] C. Michalik, T. Schmidt, M. Zavrel, M. Ansorge-Schumacher, A. Spiess, W. Marquardt, Application of the incremental identification method to the formate oxidation using formate dehydrogenase. *Chem. Eng. Sci.* 62(18–20) (2007) 5592–5597. 19th International Symposium on Chemical Reaction Engineering – From Science to Innovative Engineering—ISCRE-19.

[6] M. Mandler, I. Willner, Photosensitized NAD(P)H regeneration systems; application in the reduction of butan-2-one, pyruvic, and acetoacetic acids and in the reductive amination of pyruvic and oxoglutaric acid to amino acid, J. Chem. Soc. Perkin Trans. II (1986) 805–811.

[7] Z. Goren, N. Lapidot, I. Willner, Photocatalysed regeneration of NAD(P)H by CdS and TiO_2 semiconductors: applications in enzymatic synthesis, J. Mol. Catal. 47 (1988) 21–32.

[8] E. Siu, K. Won, C. Park, Electrochemical regeneration of NADH using conductive vanadia-silica xerogels, *Biotechnol. Prog.* 23 (2007) 293–296.

[9] E. Steckhan, Electroenzymatic synthesis, *Top. Curr. Chem.* 170 (1994) 83–111.

[10] S. Kim, S. Yun, C. Kang, Electrochemical evaluation of the reaction rate between methyl viologen mediator and diaphorase enzyme for the electrocatalytic reduction of NAD^+ and digital simulation for its voltametric responses, J. Electroanal. Chem. 465 (1999) 153–159.

[11] R. Fisher, J. Fenton, J. Iranmahboob, Electro-enzymatic synthesis of lactate using electron transfer chain biomimetic membranes, J. Membr. Sci. 177 (2000) 17–24.

[12] C. Kane, T. Tzedakis, Electrochemical microreactor for chiral syntheses using the cofactor NADH. AIChE Journal 54(5) (2008) 1365–1376. And C. Kane Conception et réalisation de microréacteurs électrochimiques – Application à la régénération électroenzymatique de NADH et potentialités en synthèse. Thèse de doctorat (PhD) de l'Université Paul Sabatier – Toulouse III, 2005.

[13] S. Kim, G.-Y. Lee, J. Lee, E. Rajkumar, J.-O. Baeg, J. Kim, Efficient electrochemical regeneration of nicotinamide cofactors using a cyclopentadienyl-rhodium complex on functionalized indium tin oxide electrodes, Electrochim. Acta 96 (2013) 141–146.

[14] A. Damian, S. Omanovic, Electrochemical reduction of NAD^+ on a polycrystalline gold electrode, J. Mol. Catal. 253 (2006) 222–233.

[15] I. Ali, A. Gill, S. Omanovic, Direct electrochemical regeneration of the enzymatic cofactor 1,4-NADH employing nano-patterned glassy carbon/Pt and glassy carbon/Ni electrodes, Chem. Eng. J. 188 (2012) 173–180.

[16] A. Garcia-Costas, A. White, W. Metcalf, Purification and characterization of a novel phosphorus-oxidizing enzyme from *Pseudomonas stutzeri* WM88, *J. Biol. Chem*. 276 (2001) 17429–17436.

[17] H. Slusarczyk, S. Felber, M. Kula, M. Pohl, Stabilization of NAD-dependent formate dehydrogenase from *Candida boidinii* by site-directed mutagenesis of cysteine residues, *Eur. J. Biochem*. 267 (2000) 1280–1289.

[18] Y. Zhang, Z. Huang, C. Du, Y. Li, Introduction of an NADH regeneration system into Klebsiella oxytoca leads to an enhanced oxidative and reductive metabolism of glycerol, Metab. Eng. 11 (2) (2009) 101–106.

[19] G.J. Balzer, C. Thakker, G.N. Bennett, K.Y. San, Metabolic engineering of Escherichia coli to minimize byproduct formate and improving succinate productivity through increasing NADH availability by heterologous expression of NAD^+-dependent formate dehydrogenase, Metab. Eng. 20 (2013) 1–8.

[20] M.A. Rauf, S.S. Ashraf, Survey of recent trends in biochemically assisted degradation of dyes, Review, Chem. Eng. J. 209 (2012) 520–530.

[21] W.A. Van der Donk, H.M. Zhao, Regeneration of cofactors for use in biocatalysis, Curr. Opin. Biotechnol. 14 (2003) 583–589.

[22] Z. Samec, W.T. Bresnaham, P.J. Elving, Theoretical analysis of electrochemical reactions involving two successive one-electron transfers with dimerization of intermediate – application to NAD^+/NADH redox couple, J. Electroanal. Chem. 133 (1982) 1–23.

[23] S. Peguin, P. Soucaille, Modulation of metabolism of *Clostridium acetobutylicum* grown in chemostat culture in a three-electrode potentiostatic system with methyl viologen as electron carrier, *Biotechnol. Bioengin*. 51 (1996) 342–348.

[24] H. Simon, J. Bader, H. Günter, S. Neumann, J. Thanos, Chiral compounds synthesized by biocatalytic reductions, Angew. Chem. Int. Ed. Engl. 24 (1985) 539–553.

[25] Y. Kashiwagi, Y. Yanagisawa, N. Shibayama, K. Nakahara, F. Kurashima, J. Anzai, T. Osa, Preparative, electroenzymatic reduction of NAD^+ to NADH on a thin poly(acrylic acid) layer-coated graphite felt electrode coimmobilizing ion-paired methyl viologen-cation-exchange polymer and diaphorase, Chem. Lett. 12 (1996) 1093–1094.

[26] T. Klotzbach, M. Watt, Y. Ansari, S. Minteer, Effects of hydrophobic modification of chitosan and Nafion on transport properties, ion-exchange capacities, and enzyme immobilization, J. Memb. Sci. 282 (2006) 276–283.

[27] T. Klotzbach, M. Watt, Y. Ansari, S. Minteer, Improving the microenvironment for enzyme immobilization at electrodes by hydrophobically modifying chitosan and Nafion polymers, J. Memb. Sci. 311 (2008) 81–88.

[28] U. Hanefeld, L. Gardossi, E. Magner, Understanding enzyme immobilization, *Chem. Soc. Rev*. 38 (2009) 453–468.

[29] Y. Gaudemer, H. Dulieu, N. Latruffe et J. Wallach, Biochimie. D. Voet, J.G. Voet, ed. J.W.a. Sons. 2. (1998), DeBoeck Université. Paris, Bruxelles.

[30] V. Zewe et, H.J. Fromm, Kinetic Studies of Rabbit Muscle Lactate Dehydrogenase, J. Biol. Chem. 237(5) (1961) 1668–1675. And V. Zewe et, H.J. Fromm, Kinetic Studies of Rabbit Muscle Lactate Dehydrogenase II-Mechanism of the reaction. Biochemistry 4 (1965) 782–92.

[31] U. Kragl, D. Vasic-Racki, C. Wandrey, Continuous processes with soluble enzymes, Ind. J. Chem. 32 (1993) 103–117.

[32] H. Groger, W. Hummel, S. Buchholz, K. Drauz, T. Nguyen, H. Husken, K. Abokitse, Practical asymmetric enzymatic reduction through discovery of a dehydrogenase-compatible biphasic reaction media, Org. Lett. 5 (2003) 173–176.

[33] M. Yalpani, L. Hall, Some chemical and analytical aspects of polysaccharide modifications. 3. Formation of branched-chain, soluble chitosan derivatives, Macromolecules 17 (1984) 272–281.

[34] J. Roche, Régénération continue du cofacteur NADH catalysée par la formate deshydrogénase immobilisée en réacteur filtre presse. Thèse de doctorat (PhD) de l'Université Paul Sabatier – Toulouse III, 2011.